

A HOLISTIC SCENARIO OF TURBULENT MOLECULAR CLOUD EVOLUTION AND CONTROL OF THE STAR FORMATION EFFICIENCY. FIRST TESTS

E. VÁZQUEZ-SEMADENI¹, J. BALLESTEROS-PAREDES¹ AND R. S. KLESSEN²

Draft version October 28, 2018

ABSTRACT

We compile a holistic scenario for molecular cloud (MC) evolution and control of the star formation efficiency (SFE), and present a first set of numerical tests of it. A *lossy* compressible cascade can generate density fluctuations and further turbulence at small scales from large-scale motions, implying that the turbulence in MCs may originate from the compressions that form them. Below a *sonic* scale λ_s , turbulence cannot induce any further subfragmentation, nor be a dominant support agent against gravity. Since progressively smaller density peaks contain progressively smaller fractions of the mass, we expect the SFE to decrease with decreasing λ_s , at least when the cloud is globally supported by turbulence. Our numerical experiments confirm this prediction. We also find that the collapsed mass fraction in the simulations always saturates below 100% efficiency. This may be due to the decreased mean density of the leftover interclump medium, which in real clouds (not confined to a box) should then be more easily dispersed, marking the “death” of the cloud. We identify two different functional dependences (“modes”) of the SFE on λ_s , which roughly correspond to globally supported and unsupported cases. Globally supported runs with most of the turbulent energy at the largest scales have similar SFEs to those of unsupported runs, providing numerical evidence of the dual role of turbulence, whereby turbulence, besides providing support, induces collapse at smaller scales through its large-scale modes. We tentatively suggest that these modes may correspond to the clustered and isolated modes of star formation, although here they are seen to form part of a continuum rather than being separate modes. Finally, we compare with previous proposals that the relevant parameter is the energy injection scale.

1. INTRODUCTION

Two of the main questions about molecular cloud (MC) structure and star formation concern the origin of molecular cloud turbulence and of the low efficiency of star formation (SFE). Indeed, the turbulent properties of molecular clouds are remarkably uniform, even in clouds without stellar energy sources (see, e.g., McKee 1999 and references therein). And, defined as the fraction of the mass in a MC that ends up in stars before the cloud is dispersed, the SFE is well known to be as low as a few percent with respect to the total cloud mass (see, e.g., Evans 1991 and references therein).

It is known that turbulence can provide additional support against global gravitational collapse (Chandrasekhar 1951; Bonazzola et al. 1987, 1992; Vázquez-Semadeni & Gazol 1995). In particular, numerical studies have suggested that turbulence is able to prevent the collapse when the energy injection scale is smaller than the Jeans length at typical core densities (Léorat, Passot & Pouquet 1990; Klessen, Heitsch & Mac Low 2000, hereafter KHM00). Simultaneously, supersonic, compressible turbulence is known to produce “fragmentation”, i.e., the formation of smaller-scale density substructures that can themselves possibly undergo local collapse (Sasao 1973; Hunter & Fleck 1982; Tohline, Bodenheimer & Christodolou 1987; Scalo 1987; Elmegreen 1993; Padoan 1995; Vázquez-Semadeni, Passot & Pouquet 1996; KHM00; Padoan et al. 2001; Heitsch, Mac Low & Klessen 2001). Padoan (1995) and KHM00 have proposed that turbulent fragmentation has an important role in determining the SFE. The

latter authors have shown that the efficiency in numerical simulations (measured as the fraction of mass in collapsed objects) increases as the energy injection scale is increased. However, this result was obtained in simulations with an idealized random forcing applied at specific scales, and ubiquitously in time and space. Instead, the turbulence in real MCs is probably injected over a wide range of scales, but at localized sites and times (Scalo 1987; Norman & Ferrara 1996; Avila-Reese & Vázquez-Semadeni 2001). In this case, the driving scale is not uniquely defined. Also, if molecular clouds form through the collisions of larger-scale streams in the more diffuse ISM (Elmegreen 1993; Ballesteros-Paredes, Vázquez-Semadeni & Scalo 1999; Vázquez-Semadeni, Ballesteros-Paredes & Klessen 2002, hereafter Paper I), then they can be part of a turbulent cascade originating from much larger scales, and thus the driving scale can be much larger than the Jeans length in the molecular clouds (Mac Low & Ossenkopf (2001). This appears inconsistent with the requirement of a driving scale smaller than the cloud’s Jeans length in order to maintain a low efficiency.

In Paper I, we have compiled a holistic scenario in which both the turbulence in molecular clouds and the SFE are part of the life cycle of MCs: *MC turbulence originates from the very process that forms the clouds*, namely colliding streams in the diffuse ISM (Elmegreen 1993; Ballesteros-Paredes et al. 1999), through bending-mode instabilities (Hunter et al. 1986; Vishniac 1994; Walder & Folini 1998; Klein & Woods 1998). In this sense, MC turbulence is part of a compressible *and lossy* cascade which may originate at intermediate scales in the Galactic disk

¹ Instituto de Astronomía, UNAM, Campus Morelia, Apdo. Postal 3-72, Morelia, Michoacán, México, e.vazquez, j.ballesteros @astrosmo.unam.mx

² Astrophysikalisches Institut Potsdam, An der Sternwarte 16, 14482 Potsdam, Germany, rklessen@aip.de

($\gtrsim 1$ kpc) from various instabilities (Parker 1966; Toomre 1964; Elmegreen 1991), supernova energy input (e.g., McCray & Snow 1979; MacLow 2002), and stellar winds (Norman & Silk 1980), and continues towards smaller scales, as the internal turbulence produces yet smaller-scale turbulent compressed layers (Kornreich & Scalo 2000). The compressible cascade has to be lossy because shocks are known to be dissipative by transferring a fraction of the energy involved directly to the dissipative scales (Kadomtsev & Petviashvili 1973). This compressible-cascade regime, however, must end at a “sonic” scale, denoted λ_s , below which the turbulence internal to the new structures becomes subsonic and therefore cannot produce any further subfragmentation (Padoan 1995). This does not necessarily imply that the dissipative (or “inner”) scale of the turbulence has been reached, but only that at this point the cascade can turn into an incompressible one. Thus, in this scenario, subsonic “cores” are the natural end of the *compressible* part of the cascade in the ISM.

When the turbulence becomes subsonic, it ceases to be a stronger source of global support than thermal pressure, and the Jeans criterion can be applied to determine whether a “core” is gravitationally unstable and should proceed to collapse (Padoan 1995), or else rebound and merge back into its environment (Elmegreen 1993; Taylor, Morata & Williams 1996; Ballesteros-Paredes et al. 1999; Vázquez-Semadeni, Shadmehri & Ballesteros-Paredes 2002). This effectively *sets an upper limit to the SFE*, because, if globally the cloud is supported by its internal turbulence, only massive enough clumps among those with sizes $l \lesssim \lambda_s$ are susceptible to local collapse (Padoan 1995). In this sense, star-forming cores constitute the intersection of the set of subsonic regions with the high-mass, super-Jeans *tail* of the mass distribution (Padoan 1995; Ballesteros-Paredes & Vázquez-Semadeni 1997; Shadmehri, Vázquez-Semadeni & Ballesteros-Paredes 2001). In particular, Padoan (1995) gave a semi-phenomenological theory for the efficiency and mass distribution of proto-stellar cores in turbulent molecular clouds (recently extended by Padoan & Nordlund 2002). In that work, however, he considered only a power-law turbulent spectrum, neglecting the necessary existence of inner and outer scales, and the role of the energy injection scale, which was proposed to be crucial by Léorat et al. (1990) and KHM00.

In this Letter, besides putting together and advancing the above global scenario, we present (§2) a first set of numerical tests supporting it, by showing that the scale λ_s indeed plays a crucial role in limiting the SFE. Clearly, this is only a partial ingredient, as the mass distribution in the flow is also expected to be crucial (Padoan 1995). Our experiments also support the notion of the dual role of turbulence in providing support to large scales while promoting small-scale collapse, as we discuss in §3, where we also give a re-interpretation of the results of KHM00 in the framework of our scenario.

2. NUMERICAL EXPERIMENTS AND RESULTS

We consider a set of 12 numerical experiments similar to those reported by KHM00. We refer the reader to that paper for details (see also Klessen & Burkert 2000, 2001). Here we just mention that they are smoothed particle hy-

drodynamics (SPH) simulations of non-magnetic turbulent flows using 205,379 particles, with self-gravity, and random forcing applied only at wavenumbers in a narrow interval $k_d - 1 \leq |\mathbf{k}| \leq k_d$, where $k_d \equiv L/\lambda_d$ is the driving wavenumber, L is the computational box size and λ_d is the driving scale. The simulations are carried out in non-dimensional units, in which there are 64 thermal Jeans masses (with respect to the mean density) in the computational box, the time unit is $t_0 = t_{\text{ff}}/1.5$, where t_{ff} is the free fall time, the sound speed is $c = 0.1$, and the mean density is $\rho_0 = 1/8$. A constant kinetic energy input rate is used, with an amplitude chosen to maintain a fixed level of turbulent kinetic energy E_t . For our analysis, the SPH data are interpolated onto a cubic grid of 128^3 cells, but note that the effective resolution of the SPH method in the density peaks (cores) is higher than that.

The runs are labeled mnemonically as $MxKy$, where x denotes the rms Mach number and y denotes the forcing wavenumber k_d . The rms Mach number M_s and the energy injection scale λ_d were taken by KHM00 as the controlling parameters in their investigation of the amount of mass in collapsed objects M_* as a function of time for several simulations. The numerical scheme allows this mass to be measured through the usage of “sink” particles, which are particles that replace a collapsing gas clump once it becomes too dense and small to be properly resolved. A sink particle inherits the combined masses of the replaced SPH particles, as well as their linear and angular momenta, and has the ability to continue accreting further SPH particles.

In order to investigate the role of the sonic scale λ_s , we consider the velocity dispersion-vs.-size relation, together with the mass-accretion histories of the simulations. The velocity dispersion-size relation we consider is not restricted to the densest, or highest-column density projected structures, as is customary in both observational (Larson 1981; see Blitz 1993 for a more recent review) and numerical (Vázquez-Semadeni, Ballesteros-Paredes & Rodríguez 1997; Ostriker, Stone & Gammie 2001; Ballesteros-Paredes & Mac Low 2002) astrophysical studies. Instead, we consider a subdivision of the whole computational box in regions of size l , and measure the velocity dispersion in all such regions. The mass accretion histories are computed as the fraction of the total mass in collapsed objects (sink particles) as a function of time.

Figure 1 shows the velocity dispersion-size relation for all runs. For every run, the solid line shows the average velocity dispersion for all regions of size l ; the “error” bars indicate the range of values of the velocity dispersion exhibited by all regions of size l . The dotted straight lines show an $R^{1/2}$ power law, and the dashed horizontal line shows the value of the sound speed. The sonic scale can be defined as that at which the solid line crosses the sound speed level, and is depicted by a vertical dotted line. Because of the large error (or, more properly, “scatter”) bars in the velocity dispersion, the sonic scale is typically defined only to within factors ~ 4 . The caveat should be mentioned that the velocity dispersion-size plots we obtain are clearly not power laws, with progressively smaller scales being progressively more deficient in turbulent kinetic energy. This is in part a consequence of the spatially varying resolution of SPH, with low resolution at low density (in voids) and high resolution at high density (in cores)

(Ossenkopf, Klessen, & Heitsch 2001), and in part a consequence of a power-law range not being expected at scales larger than λ_d for the small-driving-scale runs. In any case, the non-power-law nature of the spectrum at small scales implies that our measurements *overestimate* λ_s . We discuss the implications of this in §3.

Figure 2 shows the accretion histories for all runs. It is noteworthy that the accreted mass in most runs (except the ones with the lowest accretion rates) eventually saturates at some level. This phenomenon is extremely interesting in its own right; it clearly appears to be a real phenomenon, generally seen in simulations that allow following the evolution of the system beyond the formation of individual collapse sites through the use of sink particles (KHM00; Klessen, Burkert & Bate 2001; Klessen 2001; Bate, Bonnell & Bromm 2002). We speculate that it occurs because the local collapse events decrease the mean density of the “interclump” medium, making it more difficult to form new collapsing sites from it. Concerns that this saturation level be a numerical artifact dependent of the resolution are dispelled by fig. 6 of KHM00, which shows no clear trend of the saturation level with resolution, but only statistical scatter (different random initial conditions with the same global parameters show variations of up to a factor of 2 in the final accreted masses).

Operationally, defining the SFE is not an unambiguous task, because not all runs have had time to saturate yet (assuming they all eventually do). Given that recent studies suggest that clouds have lifetimes of only a few crossing times (Ballesteros-Paredes et al. 1999; Elmegreen 2000), we choose to define the SFE as the collapsed mass fraction after two turbulent crossing times (t_c).³ In the units of the code, these correspond to $t = 10, 12.5, 6.7$ and 4 for runs with rms Mach number $M_s = 2, 3.2, 6$, and 10 , respectively. However, for the runs with $M_s = 2$ and 3.2 , this time is longer than they have been evolved. Fortunately, the collapsed mass fractions in all these runs have saturated, and so for them we take the saturation value. Due to the statistical variation of the collapsed mass fractions mentioned above, we also put error bars of $\pm 50\%$ in the reported values of the SFE.

In order to interpret the results of the simulations, fig. 3 shows the SFE versus λ_d (a), M_s (b), and λ_s (c) for all simulations. The linear Pearson correlation coefficients for the logarithmic data in figs. 3a, 3b and 3c are respectively $0.35, -0.73$ and 0.75 , showing that indeed the SFE correlates best with the sonic scale λ_s . Note that this is in spite of the fact that the relationship between the SFE and λ_s is clearly not a power law, but instead saturates at large λ_s . A change of variable $\lambda_s \rightarrow u = -0.0038 - 0.012 \exp(-2.39 \log \lambda_s)$ gives the fit shown by the solid curve in fig. 3c, with a much tighter correlation coefficient of 0.86 . Nevertheless, the correlation with M_s is also significant. We discuss this in the next section.

3. DISCUSSION AND COMPARISON WITH PREVIOUS WORK

Although in the previous section we have fitted a smooth curve to the data in fig. 3c, actually it appears as if there are two functional dependences (“modes”) of the SFE on λ_s in this plot: for $\lambda_s \lesssim 0.03$, the SFE is nearly a power-law

on λ_s , while it is roughly constant (within a factor of 2) for $\lambda_s \gtrsim 0.03$. All the points in the former regime correspond to cases with $M_s = 6$ or 10 , which are globally supported by the turbulence, while most of the points in the latter regime correspond to $M_s = 2$ and 3.2 , which are globally unsupported. Nevertheless, the large-scale driven ($k_d = 2$) high- M_s cases appear to be at the crossover between the two regimes. This demonstrates the suggested dual nature of the turbulence (Sasao 1973; Falgarone, Puget & Péroult 1992; Vázquez-Semadeni & Passot 1999; KHM00): globally supported runs can be induced to behave as unsupported ones when the bulk of the turbulent energy is at the largest scales.

It is tempting to speculate that these two “modes” correspond to the isolated and clustered observed modes of SF. In this case, our results suggest that the two would not be physically separated modes, but simply represent a continuous transition from one functional dependence of the SFE on λ_s to the other, as the domain transits from behaving as if globally supported to behaving as if globally unsupported. We see also that, even in the globally unsupported case, the efficiency is below unity because of the saturation described above. In this case, turbulence would only provide the seeds for the internal fragmentation of the collapsing molecular cloud region (see, e.g., Klessen et al. 1998; Klessen 2001), the efficiency being more strongly dependent on stellar feedback to destroy the cloud. Further testing is necessary in order to confirm the correspondence between the two regimes found here and the observationally identified isolated and clustered modes.

Concerning the resolution of the numerical scheme, as mentioned above, λ_s is overestimated at small scales by our simulations. Moreover, in the absence of numerical diffusion, one would expect the density peaks to become narrower as well, possibly increasing the number of them that go into collapse, and thus increasing the SFE. Thus, in general we expect the correlation seen in fig. 3c to be shallower if the diffusivity is decreased. Nevertheless, we do not expect significant qualitative changes in our results.

Our reinterpretation in terms of λ_s eliminates the apparent inconsistency implied by previous works that a low SFE would seem to require a small driving scale, yet the turbulence in molecular clouds appears to be generally driven from larger scales. Indeed, our results show that a small driving scale alone is not enough to prevent collapse if it is too weak, while driving at large scales can still decrease the efficiency if it is strong enough, as pointed out by KHM00. That is, the controlling parameter is not the driving scale nor the rms Mach number alone, but instead their combined action expressed as the energy content at the sonic scale. Previous studies did not consider large-scale-driven cases with a strong enough turbulence level to decrease the SFE.

A few final remarks: 1) The mechanism sketched here is expected to operate *in addition* to any other mechanism limiting the SFE based on energy feedback from the massive stars, which can disrupt the parent cloud. 2) The occurrence of a saturation of the accreted mass implies that clouds could not achieve 100% SFE even if they had arbitrarily large amounts of time available, provided the turbulence level is kept constant. This is because *local* collapse

³ We thank the referee for suggesting this criterion.

uses up part of the mass, rendering the remaining gas more diffuse and easy to disperse. Thus, *partial dispersion may also be part of the natural course of evolution of molecular clouds*. 3) In this work we have neglected the effect of the magnetic fields. Although their effect certainly must be incorporated in a full theory, the mechanism discussed here is capable of regulating the SFE without relying on their presence, depending only on the spatial redistribution of the physical quantities in a compressible turbulent flow. This is particularly relevant upon recent suggestions that molecular clouds may be super-Alfvénic (Padoan & Nordlund 1999) and that cores are in general supercritical

(Nakano 1998; Hartmann, Ballesteros-Paredes & Bergin 2001; Bourke et al. 2001; Crutcher, Heiles & Troland 2002).

We thank L. Hartmann and the referee, P. Padoan, for useful suggestions. We acknowledge financial support from Conacyt grants 27752-E to E.V.-S. and I39318-E to J.B.-P., and from the Emmy Noether Program of the Deutsche Forschungsgemeinschaft (KL1358/1) and the Center for Star Formation Studies (NASA-Ames, UC Berkeley, and UC Santa Cruz), to R.S.K.

REFERENCES

- Avila-Reese, V. & Vázquez-Semadeni, E. 2001, ApJ 553, 645
 Ballesteros-Paredes, J. & Vázquez-Semadeni 1997, in 7th Annual Astrophysics Conference in Maryland. Star Formation, Near and Far", ed. S. Holt y L. Mundy (New York: AIP Press), 81
 Ballesteros-Paredes, J., Vázquez-Semadeni, E. & Scalo, J. 1999, ApJ 515, 286
 Ballesteros-Paredes, J. & Mac Low, M.-M. 2002, ApJ 570, 734
 Bate, M. R., Bonnell, I. A. & Bromm, V. 2002, MNRAS 336, 705
 Blitz, L. 1993, in Protostars and Planets III, eds. E. Levy and J. Lunine (Tucson: University of Arizona Press), 125
 Bonazzola, S., Heyvaerts, J., Falgarone, E., Péroult, M., Puget, J. L. 1987, A&A 172, 293
 Bonazzola, S., Péroult, M., Puget, J. L., Heyvaerts, J., Falgarone, E., Panis, J. F. 1992, Journ. Fluid Mech. 245, 1
 Bourke, T. L., Myers, P. C., Robinson, G. & Hyland, A. R. 2001, ApJ 554, 916
 Chandrasekhar, S. 1951, Proc. Roy. Soc. London 210, 26
 Crutcher, R., Heiles, C. & Troland, T. 2002, in Simulations of Magnetohydrodynamic Turbulence in Astrophysics, ed. T. Passot & E. Falgarone (Dordrecht: Springer), in press
 Elmegreen, B. G. 1991, ApJ 378, 139
 Elmegreen, B. G. 1993, ApJ 419, L29
 Evans, N. J. II 1991, in Frontiers of Stellar Evolution, ed. D. L. Lambert (San Francisco: Astronomical Society of the Pacific), 45
 Falgarone, E., Puget, J.-L. & Péroult, M. 1992, A&A 257, 715
 Hartmann, L., Ballesteros-Paredes, J. & Bergin, E. A. 2001, ApJ 562, 852
 Hartmann, L. 2002, ApJ, in press (astro-ph/0211021)
 Heitsch, F., Mac Low, M.-M. & Klessen, R. S. 2001, ApJ, 547, 280
 Hunter, J. H., Jr., & Fleck, R. C., Jr. 1982, ApJ 256, 505
 Hunter, J., Sandford, M. T., Whitacker, R. W., & Klein, R. I. 1986, ApJ, 305, 309
 Kadomtsev, B. B. & Petviashvili, V. I. 1973, Sov. Phys. Dokl. 18, 115
 Klein, R. I. & Woods, T. 1998, ApJ 497, 777
 Klessen, R. S. 2001, ApJ, 556, 837
 Klessen, R. S. & Burkert, A. 2000, ApJS, 128, 287
 Klessen, R. S. & Burkert, A. 2001, 549, 386
 Klessen, R. S. Burkert, A. & Bate, M. R. 1998, ApJ, 501, L205
 Klessen, R. S., Heitsch, F. & Mac Low, M.-M. 2000, ApJ 535, 887 (KHM00)
 Kornreich, P. & Scalo, J. 2000, ApJ 531, 366
 Larson, R. B. 1981, MNRAS 194, 809
 Léorat, J., Passot, T. & Pouquet, A. 1990, MNRAS 243, 293
 Mac Low, M.-M. & Ossenkopf 2002, A&A 353, 339
 McCray, R. & Snow, T. P. Jr. 1979, ARAA 17, 213
 McKee, C. F. 1999, in The Origin of Stars and Planetary Systems, ed. J. L. Charles & D. K. Nikolaos (Dordrecht: Kluwer), 29
 Nakano, T. 1998, ApJ 494, 587
 Norman, C. & Silk, J. 1980
 Norman, C. & Ferrara, A. 1996, ApJ 467, 280
 Ossenkopf, V., Klessen, R. S. & Heitsch, F. 2001, Å, 379, 1005
 Ostriker, E. C., Stone, J. M. & Gammie, C. F. 2001, ApJ
 Padoan, P. 1995, MNRAS 277, 377
 Padoan, P. & Nordlund, Å 1999, ApJ 526, 279
 Padoan, P. & Nordlund 2002, ApJ 576, 870
 Padoan, P., Juvela, M., Goodman, A. A. & Nordlund, Å. 2001, ApJ 553, 227
 Parker, E. N. 1966, ApJ 145, 811
 Sasao, T. 1973, PASJ 25, 1
 Scalo, J. 1987, in Interstellar Processes, eds. D.J. Hollenbach & H.A. Thronson (Dordrecht: Reidel), p. 349
 Shadmehri, M., Vázquez-Semadeni, E. & Ballesteros-Paredes, J. 2001, in "Seeing Through the Dust", eds. R. Taylor, T. Landecker and A. Willis (San Francisco: ASP), in press, astro-ph/0111574
 Taylor, S.D., Morata, O. & Williams, D.A. 1996, A&A 313, 269
 Tohline, J. E., Bodenheimer, P. H. & Christodolou, D. M. 1987, ApJ 322, 787
 Toomre, A. 1964, ApJ 139, 1217
 Vázquez-Semadeni, E. & Gazol, A. 1995, A&A 303, 204
 Vázquez-Semadeni, E., Passot, T. & Pouquet, A. 1996, ApJ 473, 881
 Vázquez-Semadeni, E., Ballesteros-Paredes, J. & Rodríguez, L. F. 1997, ApJ 474, 292
 Vázquez-Semadeni, E. & Passot, T., in Interstellar Turbulence, eds. J. Franco and A. Carramiñana (Cambridge: Cambridge University Press), 223
 Vázquez-Semadeni, E., Shadmehri, M. & Ballesteros-Paredes, J. 2002, submitted to ApJ (astro-ph/0208245)
 Vázquez-Semadeni, E. Ballesteros-Paredes, J. & Klessen, R. 2002, in Galactic Star Formation Across the Mass Spectrum, ed. J. de Buizer (San Francisco: ASP), in press (astro-ph/0206038)
 Vishniac, E. 1994, ApJ 428, 186
 Walder, R. & Folini, D. 1998 A&A 330L, 21

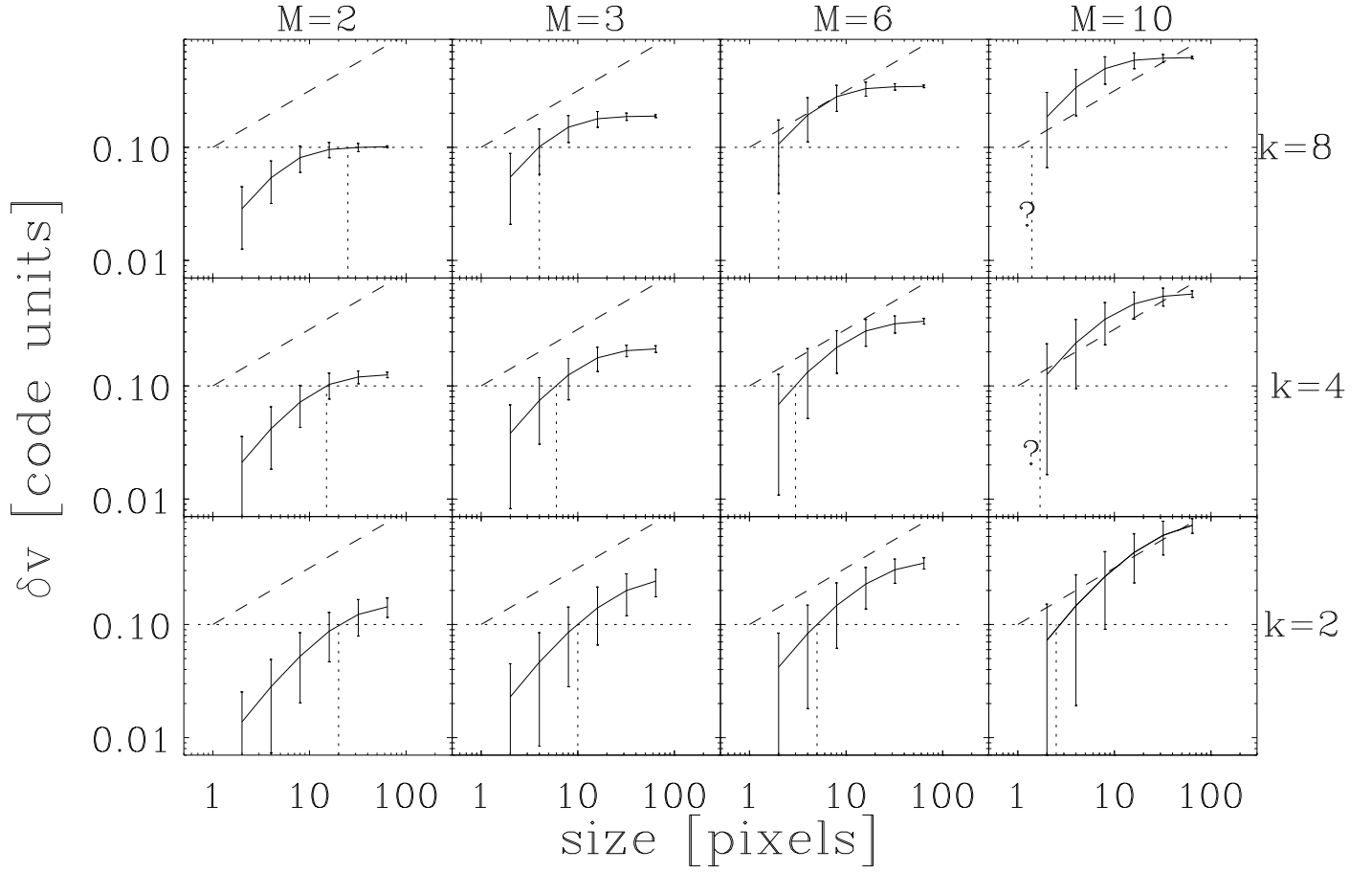


FIG. 1.— Velocity dispersion Δv versus size R for all runs considered in this paper (solid line). The nomenclature of the runs indicates their nominal rms Mach number M_s and the driving wavenumber k_d . The dashed line shows an $R^{1/2}$ law, the horizontal dotted line shows the value of the sound speed, and the vertical line marks the sonic scale. The error bars indicate the scatter of the around the mean value of Δv .

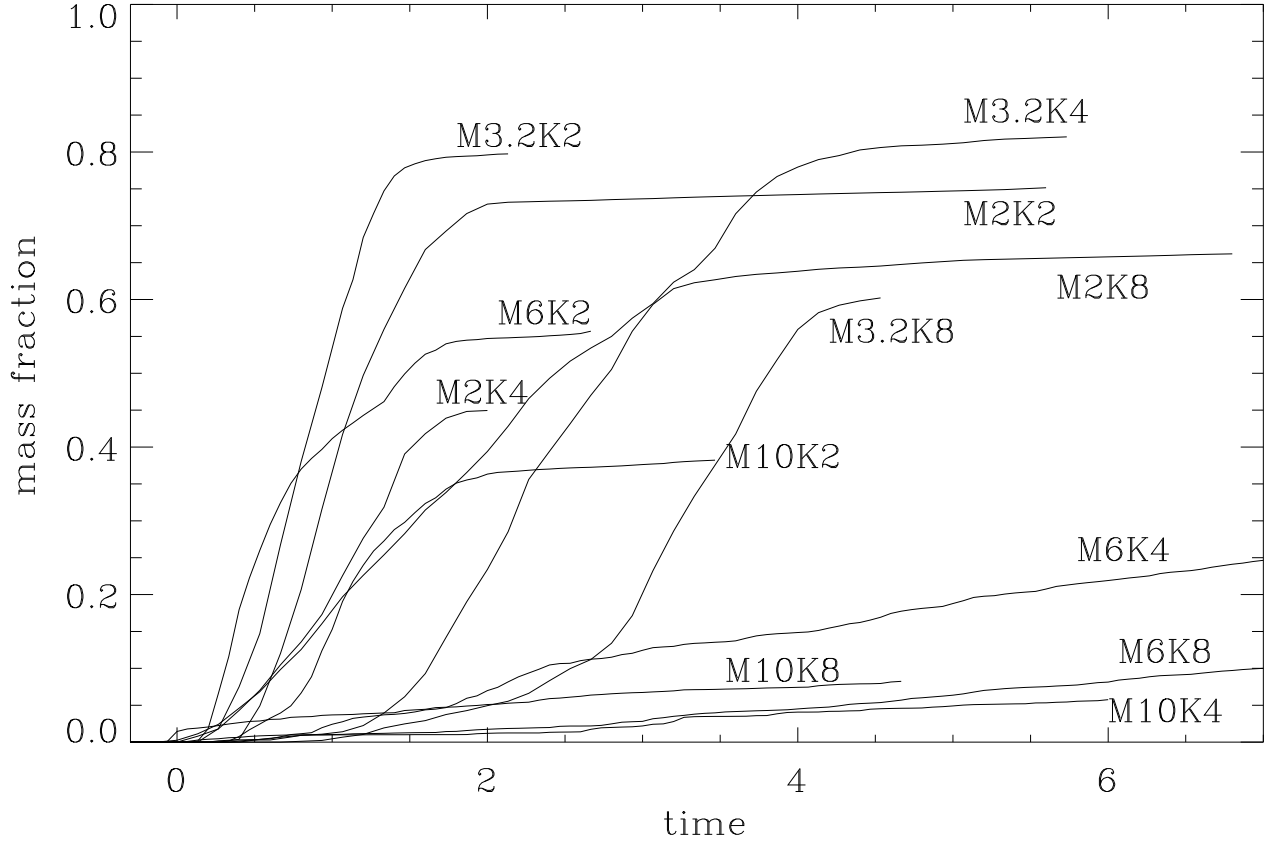


FIG. 2.— Evolution of the collapsed mass fraction for all runs. We define the star formation efficiency (SFE) as the collapsed mass fraction at time $t = 4, 6.7$ for runs with $M_s = 10, 6$, respectively, and as the saturation value for runs with $M_s = 3.2$ and 2.

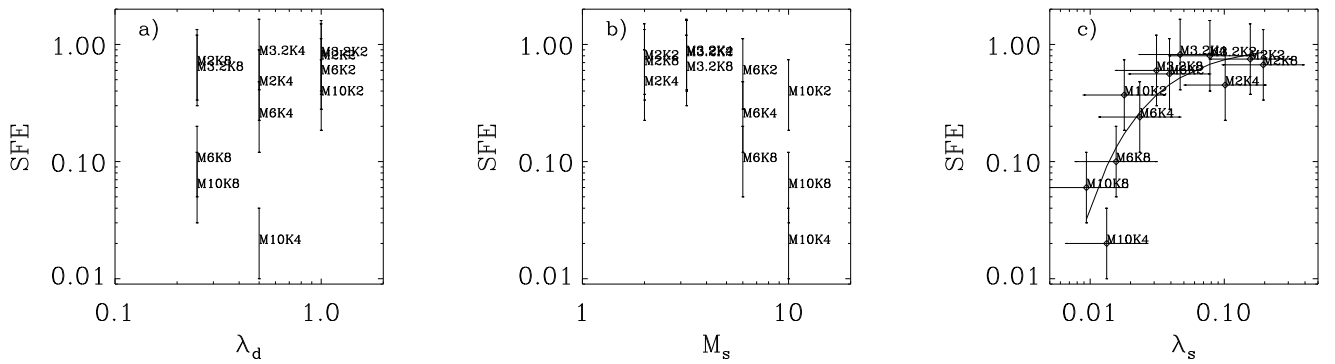


FIG. 3.— Dependence of the SFE on the driving length λ_d (a), the rms Mach number M_s (b) and the sonic scale λ_s in units of the box size (c). The error bars in the SFE indicate the statistical variation among different realizations with the same global parameters found by KHM00.